Micromotion-Induced Limit to Atom-Ion Sympathetic Cooling in Paul Traps

Marko Cetina,[*] Andrew T. Grier, and Vladan Vuletić

*Department of Physics, MIT-Harvard Center for Ultracold Atoms, and Research Laboratory of Electronics,
Massachusetts Institute of Technology, Cambridge, Massachusetts 02139, USA*
(Received 12 May 2012; published 19 December 2012)

We present, and derive analytic expressions for, a fundamental limit to the sympathetic cooling of ions in radio-frequency traps using cold atoms. The limit arises from the work done by the trap electric field during a long-range ion-atom collision and applies even to cooling by a zero-temperature atomic gas in a perfectly compensated trap. We conclude that in current experimental implementations, this collisional heating prevents access to the regimes of single-partial-wave atom-ion interaction or quantized ion motion. We determine conditions on the atom-ion mass ratio and on the trap parameters for reaching the *s*-wave collision regime and the trap ground state.

The combination of cold trapped ions and atoms [1–8] constitutes an emerging field that offers unexplored possibilities for the study of quantum gases. New proposed phenomena and tools include sympathetic cooling to ultracold temperatures [9,10], charge transport in cold atomic gases [11,12], dressed ion-atom states [13–16], local high-resolution probes [17,18], and ion-atom quantum gates [19,20].

In contrast to conservative atom traps, Paul traps employ radio-frequency (rf) electric fields to create a time-averaged secular trapping potential for the ion [21]. The rf field can pump energy into the system if the ion's driven motion is disturbed, e.g., by a collision with an atom [22]. The kinetic behavior of an ion in a neutral buffer gas has been observed in numerous experiments [23–30]. The ion's equilibrium energy distribution was predicted analytically [31], as well as using Monte Carlo techniques [26,27,32,33], and recently a quantum mechanical analysis has been performed [34]. For atom-ion mass ratios below a critical value, the ion is predicted to acquire a stationary nonthermal energy distribution with a characteristic width set by the coolant temperature [33].

The rf field drives micromotion of the ion at the rf frequency. At any position and time, the ion's velocity can be decomposed into the micromotion velocity and the remaining velocity of the secular motion. Consider the simple case of a sudden collision with an atom that brings the ion to rest, a process which in a conservative trap would remove all kinetic energy. Immediately after such a collision, the ion's secular velocity is equal and opposite to the micromotion velocity at the time of the collision. This implies that the ion's secular motion can be increased even in a collision that brings it momentarily to rest. Hence, for cooling by an ultracold atomic gas [3,4], the energy scale of the problem is no longer set by the atoms' temperature but by the residual rf motion of the ion, caused, e.g., by phase errors of the rf drive or by dc electric fields which displace the trap minimum from the rf node [35]. Such technical imperfections have limited

sympathetic cooling so far, with the lowest inferred ion temperature on the order of 0.5 mK [7]. Full quantum control in these systems [19,20], however, likely requires access to the smaller temperature scales $\hbar\omega/k_B \sim 50~\mu$K for the trap zero-point motion and $E_s/k_B \sim 50$ nK for the *s*-wave collision threshold [11].

In this Letter, we show that even with the atomic gas at zero temperature and in a perfectly dc- and rf-compensated Paul trap, a fundamental limit to sympathetic atom-ion cooling arises from the electric field of the atom when polarized by the ion, or equivalently, the long-range ion-atom interaction. The approaching atom displaces the ion from the rf node leading to micromotion, whose interruption causes heating. A second nonconservative process arises from the nonadiabatic motion of the ion relative to the rf field due to the long-range atom-ion potential; here, the trap can do work on the ion and increase its total energy. We find that, in realistic traps, the work done by the rf field dominates the effect of the sudden interruption of the ion's micromotion and leads to an equilibrium energy scale that, for all but the lightest atoms and heaviest ions, substantially exceeds both the *s*-wave threshold E_s and the trap vibration energy $\hbar\omega$. Our analysis shows that current atom-ion experiments [1–8] will be confined to the regimes of multiple partial waves and vibrational quanta and indicates how to choose particle masses and trap parameters in order to achieve full quantum control in future experiments. Our results are supported by numerical calculations that furthermore reveal that in those collisions where the rf field removes energy from the system, the atom becomes loosely bound to the ion, leading to multiple subsequent close-range collisions until enough energy is absorbed from the rf field to eject the atom and heat the ion.

We consider a classical model and later confirm that the energies obtained from this model are consistent with a classical description. An atom of mass m_a approaches from infinity to an ion of mass m_i held stationary in the center of an rf quadrupole trap. At sufficiently low collision energies, the

angular-momentum barrier will be located far from the collision point, and, once it is passed, the collision trajectory will be nearly a straight line. We initially assume this trajectory to be along an eigenaxis of the rf trap, resulting in a true one-dimensional collision in the potential $V(r_i, r_a, t) = e\mathcal{E}(r_i, t)r_i/2 + U(r)$, where e is the ion's charge, r_i and r_a are the ion and atom locations, respectively, $r = r_i - r_a$ is the ion-atom distance, and $\mathcal{E}(r_i, t) = gr_i \cos(\Omega t + \phi)$ is the rf electric field of the ion trap at frequency Ω, parametrized by its quadrupole strength g. The ion-atom interaction potential at large distances is $U(r) = -C_4/(2r^4)$ [11] with C_4 the atom's polarizability and is modeled as a hard-core repulsion at some small distance. Since in a three-dimensional collision the atom can approach the ion along directions that are perpendicular to the rf field or where the rf field vanishes, we expect our analysis to overestimate the heating by a factor of order unity, which we address below.

As the ion is pulled from the trap origin by the long-range interaction U with the approaching atom, the oscillating electric field $\mathcal{E}$ causes it to execute sinusoidal micromotion with amplitude $qr_i/2$, where $q = 2eg/(m_i\Omega^2)$ is the unitless Mathieu parameter. As long as the relative ion-atom motion remains slow compared to the ion's average rf micromotion velocity $v_{\mu m}$, the ion's equations of motion will remain linear, and its secular motion will be governed by an effective conservative potential $V_s = \frac{1}{2}m_i\omega^2 r_i^2 + U(r)$, where $\omega \approx q\Omega/2^{3/2}$ is the ion's secular frequency. Associated with V_s are the characteristic length scale $R = C_4^{1/6}/(m_i\omega^2)^{1/6}$ at which the interaction potential U is equal in magnitude to the trap harmonic potential, time scale $T = 2\pi/\omega$, and energy scale $E_R = \frac{1}{2}m_i\omega^2 R^2 = \frac{1}{2}(m_i^2\omega^4 C_4)^{1/3}$.

In collisions with light atoms, $m_a < m_i$, we expect the ion to remain close to the trap origin. In this case, the ion-atom distance $r(t)$ is governed solely by the motion of the atom in the ion-atom potential U,

$$r(t) \approx (9C_4/\mu)^{1/6}|t|^{1/3}, \tag{1}$$

where the collision occurs at time $t = 0$, and $\mu = m_i m_a/(m_i + m_a)$ is the reduced mass. The ion's displacement r_c from the trap center during the hard-core collision can be estimated by integrating the effect of the force $2C_4/r^5$ exerted by the atom on the ion trapped in its secular potential, yielding $r_c \approx 1.11(m_a/m_i)^{5/6}R$. In collisions with heavy atoms ($m_i < m_a$), the ion responds quickly to minimize the total secular potential until, at $(r_i, r_a) = (0.29, 1.76)R$, its deformed equilibrium position becomes unstable and the light ion quickly falls towards the atom with the collision occurring at the ion displacement $r_c \approx 1.76R$. For a general mass ratio, $r_c/R = \tilde{r}_c(q, m_a/m_i)/(1 + m_i/m_a)^{5/6}$, where $1 < \tilde{r}_c < 2$.

Around the collision point r_c, the energy of the system will change as long as the ion moves nonadiabatically relative to the rf field, including the interval $-t_1 < 0 < t_1$ around the collision at $t = 0$, during which the ion's velocity $\dot{r}_i$ is greater than its average micromotion velocity $v_{\mu m} \approx \omega r_c$. Here, the trap rf field acts as a time-dependent perturbation to the ion-atom potential, doing work on the ion equal to

$$W = e\int_{-t_1}^{t_1} \mathcal{E}(r_i(t), t) \cdot \dot{r}_i(t)dt. \tag{2}$$

The change in the system's energy depends on rf phase ϕ at the time of the close-range collision, reaching the maximal value $W_{\max}$ for $\phi = \phi_{\max}$. For $\dot{r}_i \gg v_{\mu m}$, we may neglect the effect of the electric field on the ion's trajectory and approximate the ion's position using the free collision trajectory $r(t)$, Eq. (1), as $r_i \approx r_c - m_a r/(m_i + m_a)$. The work done by the rf field can then be written as $W \approx Q \sin\phi$, where

$$Q = W_0 \int_{-\Omega t_1}^{\Omega t_1} \left[\frac{\sqrt{2}\tilde{r}_c}{(3|\tau|)^{2/3}} - \frac{q^{1/3}}{(3|\tau|)^{1/3}}\right]\sin|\tau|d\tau, \tag{3}$$

and

$$W_0 = 2\left(\frac{m_a}{m_i + m_a}\right)^{5/3}\left(\frac{m_i^2\omega^4 C_4}{q^2}\right)^{1/3} \tag{4}$$

is the characteristic scale for the work done on the ion by the rf field. The maximal energy gain $W_{\max} \approx Q$ occurs for $\phi = \phi_{\max} \approx \pi/2$, corresponding to the rf field changing sign at the time of the collision. The nonadiabatic condition $|\dot{r}_i| > |v_{\mu m}|$ is equivalent to $3q\Omega t < (2/\tilde{r}_c)^{3/2}$, which, for the practically relevant values of $q < 0.5$, will always include the region $|\Omega t| < 0.8$ where the dominant contribution to the integral in (3) occurs. Consequently, we may extend the limits of integration to $\pm\infty$ to obtain $Q/W_0 \approx 1.82\tilde{r}_c - 1.63q^{1/3}$, implying $0.7 < Q/W_0 < 2.8$ for $q < 0.5$ and at all mass ratios. Under the same conditions, Q is at least three times larger than the ion's average micromotion energy at the collision point $E_{\mu m} \approx m_i v_{\mu m}^2/2$ and the gradual energy change (2) dominates the effect of the sudden interruption of the ion's micromotion. Intuitively, at low collision energies, the ion-atom potential dominates for a longer time during which the rf field does more work. Since the trap electric field must be increased for higher rf frequencies to preserve the ion secular potential, the heating increases with a decrease in the Mathieu parameter ($Q > 15E_{\mu m}$ for $q < 0.1$).

Since W corresponds to the difference in the work done by the rf field during the incoming and outgoing parts of the collision, the energy change will depend on the phase ϕ of the rf field at the time of the hard-core collision. For $0 < \phi < \pi$, the rf field accelerates the collision partners towards each other, increasing the system energy; for $\pi < \phi < 2\pi$, the rf field opposes the collision, does negative work and causes the atom to be bound to the ion with binding energy on the order of $-W_0$ (Fig. 1). Since the r^{-4} potential has no stable orbits, bound ion-atom trajectories will include further close-range collisions. Depending on the rf phase during each subsequent collision, the system
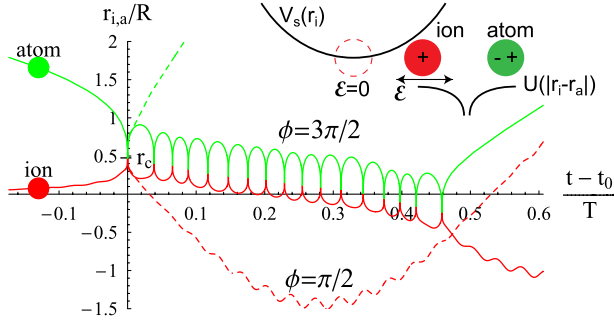
FIG. 1 (color online). Trajectories of an ion $r_i(t)$ and an atom $r_a(t)$ during a classical one-dimensional low-energy collision. The atom of mass m_a approaches the ion of mass $m_i = 2m_a$ held in the center of a rf trap with secular frequency $\omega = 2\pi/T$ and Mathieu parameter $q = 0.1$, leading to a hard-core collision at $r_i = r_a = r_c$, $t = 0$ and rf phase ϕ. For $\phi = \pi/2$ (dotted lines), the rf field adds energy to the system, causing heating. For $\phi = 3\pi/2$ (solid lines), the rf field removes energy, binding the atom to the ion and causing further collisions at various rf phases until enough energy is accumulated to eject the atom.

will gain or lose energy on the order of W_0, leading to a random walk in energy until the atom finally unbinds. Then ΔE depends sensitively on the rf phases at each hard-core collision spaced in time by many rf cycles, leading to a sharp dependence of ΔE on the rf phase ϕ during the initial collision for $\pi < \phi < 2\pi$ (Fig. 2). Using the approach below, we calculate the net average energy gain for $0 < \phi < 2\pi$ and $m_a/m_i = 1/2$, $q = 0.1$ as $\langle\Delta E\rangle = 1.0W_0$.

To verify the above heating model, we numerically calculated classical trajectories of low-energy one-dimensional collisions as a function of ϕ, m_a/m_i and q (Figs. 2 and 3). The ion was initially held at the trap center while the atom followed the analytic trajectory (1). At a critical ion-atom distance r_0, the ion was displaced so that the trap's secular force would balance the atom's attraction, while keeping its
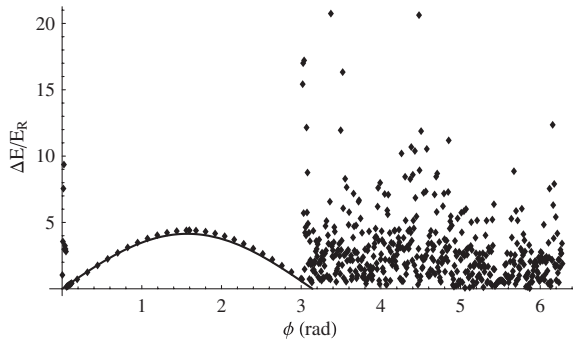

FIG. 3. Maximal energy gain $W_{\max}$ in a low-energy one-dimensional ion-atom collision as a function of the atom/ion mass ratio m_a/m_i with Mathieu parameter $q = 0.1$ (a) and as a function of q with $m_a/m_i = 1/2$ (b). Data points are numeric calculations. The solid lines correspond to $W_{\max} = Q$, while the dashed lines represent $W_{\max} = W_0$.

velocity zero. Choosing $r_0 = 3.8(1 + m_i/m_a)^{1/3}R$ ensured that for all the trap parameters in this Letter, the ion's initial micromotion energy was smaller than $10^{-5}W_0$ and both the atom's kinetic energy and $U(r_0)$ were smaller than $10^{-2}W_0$. The equations of motion were integrated using the Dormand-Prince explicit Runge-Kutta method: away from collision points, the integration variable was time while near the collisions the ion-atom distance r was used with a hard-core radius $\epsilon = 10^{-3}(1 + m_i/m_a)^{1/3}R$. The integration was stopped when the atom reached a distance $r_a = 2.1r_0$ much larger than the ion motion, at which point the total secular energy of the system was evaluated. We confirmed the accuracy of our integration by replacing the rf potential with a time-independent secular potential and confirming energy conservation at the level of $10^{-3}W_0$.

Figures 3(a) and 3(b) show the numerically calculated maximal energy gain $W_{\max}$ in the initial collision as a function

FIG. 2. Change ΔE in the total secular energy of a colliding ion-atom system ($m_a/m_i = 1/2$, $q = 0.1$), as a function of the rf phase ϕ during the first hard-core collision. For $0 < \phi < \pi$, the system undergoes only one collision with energy gain comparable to the analytic prediction (3) (solid line). For $\pi < \phi < 2\pi$, the atom is bound and undergoes several collisions with the ion before eventually escaping.
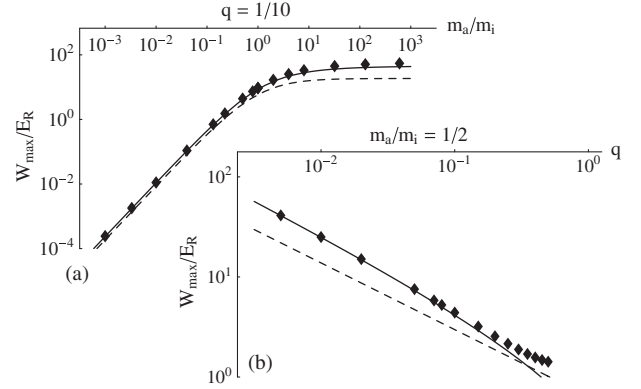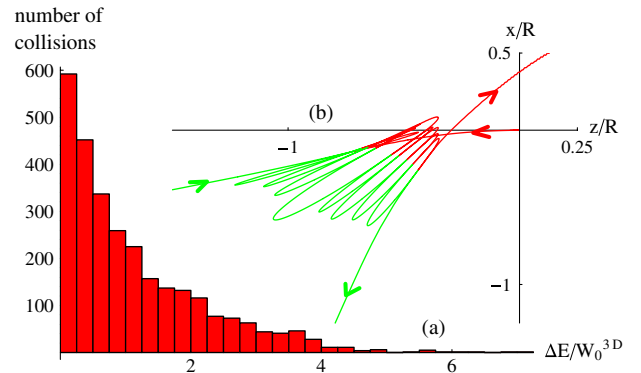

FIG. 4 (color online). (a) Distribution of numerically computed secular energy gains in 2883 random low-energy collisions between a free ^{87}Rb atom and a ^{174}Yb$^+$ ion held in the three-dimensional trap from Ref. [2], in units of the three-dimensional micromotion heating energy scale $W_0^{3D} = 4\,W_0/(3\pi)$. Inset (b) shows a sample ion-atom collision trajectory.

TABLE I.   The quantum s-wave energy limit (E_s), the corresponding radial dc electric field E_{DC}^s at which the ion micromotion energy is equal to E_s, the ion trap vibrational quantum ($\hbar\omega$), and the micromotion-induced energy scale W_0 in various ion-atom systems. The $Yb^+ + Rb$ and $Ba^+ + Rb$ systems have a sufficiently large ratio of elastic to inelastic collisions to permit cooling [4,8]. For $Yb^+ + Yb$ and $Rb^+ + Rb$, charge exchange collisions are endothermic for certain isotope combinations. The $Yb^+ + Ca$ system exhibits a very large inelastic collision rate.

Ion	Atom	q	E_s/k_B (nK)	E_{DC}^s (mV/m)	$\hbar\omega/k_B$ (μK)	W_0/k_B (μK)
$^{174}Yb^+$	^{87}Rb [2]	0.013	44	4.6	9.6	540
$^{87}Rb^+$	^{87}Rb [7]	0.24	79	7.7	17	210
$^{138}Ba^+$	^{87}Rb [4]	0.11	52	4.5	9.6	150
$^{40}Ca^+$	^{87}Rb [6]	0.20	200	2.6	5.3	50
$^{174}Yb^+$	^{172}Yb [1]	0.14	44	1.6	3.2	41
$^{174}Yb^+$	^{40}Ca [5]	0.25	270	14	12	32
$^{174}Yb^+$	^{23}Na	0.30	710	4.7	2.4	1.5
$^{174}Yb^+$	^7Li	0.30	6400	14	2.4	0.24

of m_a/m_i and q. For $q \lesssim 0.1$, the calculated W_{max} is within 30% of the analytic prediction $W_{max} = Q$; for $q = 0.5$, $m_a/m_i = 1/2$, W_{max} increases to $1.7Q$, partly because the analytic result does not include the micromotion interruption. The heating is insensitive to the hard-core radius: a tenfold increase or decrease in ϵ changes W_{max} by less than 1%. Our results are also robust with respect to the initial conditions: the average energy gain in Fig. 2 changes by less than 5% if the ion is started at rest at the trap center and the atom is started at rest a distance R away.

In three-dimensional linear quadrupole rf traps, the electric field $\mathcal{E}$ and the ion position r_i in (2) are vectorial quantities. Assuming that the collision trajectory is still nearly one-dimensional, averaging over the atom's approach direction rescales the work done by the rf field, Eq. (2), by $4/(3\pi)$, leading to a natural three-dimensional heating scale $W_0^{3D} = 4W_0/(3\pi)$. To check this, numerical simulations were done for the three-dimensional quadrupole rf trap from Ref. [2]. We considered cold ^{87}Rb atoms that have passed the angular momentum barrier at a large distance and are colliding head-on with a $^{174}Yb^+$ ion from a random direction and at a random time. The initial conditions were chosen by analogy to the one-dimensional case. Figure 4(b) shows a sample ion-atom trajectory including multiple collisions. Due to a difference in the axial and radial frequencies of the ion trap, the collision trajectory precesses about the y axis, while remaining nearly one-dimensional close to the collision points. A histogram of the final system energies E after the atom is ejected to infinity is shown on Fig. 4(a), with an average energy gain of $0.9W_0^{3D}$, confirming the heating scale W_0^{3D}.

Table I shows W_0 together with the s-wave threshold energy $E_s = \hbar^4/(2\mu^2 C_4)$ and the energy $\hbar\omega$ of a trap vibrational quantum in various experimental systems. In the current systems [1–8], atom number per characteristic volume R^3 is much smaller than one, while the atoms' kinetic energy is much smaller than W_0, and we expect binary ion-atom collisions to be well described by our model. Given the typical

duration of a collision of about $T/2$ and typical ion-atom collision rate coefficients [7], few-body effects, including three-body recombination into loosely bound molecular ions, are expected at critical atom densities on the order of $n_c \sim 10^{14}$ cm^{-3}. As their dynamics becomes fast relative to the rf frequency, ion-atom states with binding energies several times larger than W_0 may experience significantly decreased heating [34]. On the other hand, three-body processes have been observed to induce strong loss into electronically bound states [7]. Thus, the best sympathetic cooling is expected in the density regime $n < n_c$, where it is limited by the two-body energy scale W_0 to temperatures $T_{min} \sim W_0/k_B$. In the present systems, W_0 is more than one (almost three) orders of magnitude larger than the trap vibrational quantum (s-wave scattering limit).

Since, for light atoms, the ratios of heating to the s-wave collision threshold and to the trap vibration quantum scale as $W_0/\hbar\omega \propto (\omega C_4)^{4/3} m_a^{11/3}/m_i$ and $W_0/(\hbar\omega) \propto (\omega C_4)^{1/3} m_a^{5/3}/m_i$, respectively, our model predicts that micromotion heating could be mitigated using light atoms and heavy ions trapped in weak rf traps, limited by the control of dc fields (since $E_{DC}^s \propto \omega$). In particular, with control over the dc electric fields on the order of 10 mV/m, an order of magnitude better than current state-of-the-art [7], the Yb^+/Li system might enter the s-wave regime. Heating could also be decreased by employing Raman transitions to produce sufficiently deeply bound molecular ions [34]. Another option may be the use of an optical trap for the ion, as was recently demonstrated [36].

[1] A. T. Grier, M. Cetina, F. Oručević, and V. Vuletić, Phys. Rev. Lett. **102**, 223201 (2009).
[2] C. Zipkes, S. Palzer, C. Sias, and M. Köhl, Nature (London) **464**, 388 (2010).

[3] C. Zipkes, S. Palzer, L. Ratschbacher, C. Sias, and M. Köhl, Phys. Rev. Lett. **105**, 133201 (2010).

[4] S. Schmid, A. Härter, and J. H. Denschlag, Phys. Rev. Lett. **105**, 133202 (2010).

[5] W. G. Rellergert, S. T. Sullivan, S. Kotochigova, A. Petrov, K. Chen, S. J. Schowalter, and E. R. Hudson, Phys. Rev. Lett. **107**, 243201 (2011).

[6] F. H. J. Hall, M. Aymar, N. Bouloufa-Maafa, O. Dulieu, and S. Willitsch, Phys. Rev. Lett. **107**, 243202 (2011).

[7] A. Härter, A. Krükow, A. Brunner, W. Schnitzler, S. Schmid, and J. H. Denschlag, Phys. Rev. Lett. **109**, 123201 (2012).

[8] L. Ratschbacher, C. Zipkes, C. Sias, and M. Köhl, Nat. Phys. **8**, 649 (2012).

[9] W. W. Smith, O. P. Makarov, and J. Lin, J. Mod. Opt. **52**, 2253 (2005).

[10] E. R. Hudson, Phys. Rev. A **79**, 032716 (2009).

[11] R. Côté and A. Dalgarno, Phys. Rev. A **62**, 012709 (2000).

[12] R. Côté, Phys. Rev. Lett. **85**, 5316 (2000).

[13] R. Côté, V. Kharchenko, and M. D. Lukin, Phys. Rev. Lett. **89**, 093001 (2002).

[14] P. Massignan, C. J. Pethick, and H. Smith, Phys. Rev. A **71**, 023606 (2005).

[15] J. Goold, H. Doerk, Z. Idziaszek, T. Calarco, and T. Busch, Phys. Rev. A **81**, 041601(R) (2010).

[16] B. Gao, Phys. Rev. Lett. **104**, 213201 (2010).

[17] C. Kollath, M. Köhl, and T. Giamarchi, Phys. Rev. A **76**, 063602 (2007).

[18] Y. Sherkunov, B. Muzykantskii, N. d'Ambrumenil, and B. D. Simons, Phys. Rev. A **79**, 023604 (2009).

[19] Z. Idziaszek, T. Calarco, and P. Zoller, Phys. Rev. A **76**, 033409 (2007).

[20] H. Doerk, Z. Idziaszek, and T. Calarco, Phys. Rev. A **81**, 012708 (2010).

[21] D. Leibfried, R. Blatt, C. Monroe, and D. Wineland, Rev. Mod. Phys. **75**, 281 (2003).

[22] F. G. Major and H. G. Dehmelt, Phys. Rev. **170**, 91 (1968).

[23] H. Schaaf, U. Schmeling, and G. Werth, Appl. Phys. **25**, 249 (1981).

[24] L. S. Cutler, R. P. Giffard, and M. D. McGuire, Appl. Phys. B **36**, 137 (1985).

[25] M. D. N. Lunney, F. Buchinger, and R. B. Moore, J. Mod. Opt. **39**, 349 (1992).

[26] F. Herfurth, J. Dilling, A. Kellerbauer, G. Bollen, S. Henry, and H. Kluge, Nucl. Instrum. Methods Phys. Res., Sect. A **469**, 254 (2001).

[27] A. Kellerbauer, T. Kim, R. B. Moore, and P. Varfalvy, Nucl. Instrum. Methods Phys. Res., Sect. A **469**, 276 (2001).

[28] M. Green *et al.*, Phys. Rev. A **76**, 023404 (2007).

[29] J. Mikosch, U. Frühling, S. Trippel, D. Schwalm, M. Weidemüller, and R. Wester, Phys. Rev. Lett. **98**, 223001 (2007).

[30] B. Flatt *et al.*, Nucl. Instrum. Methods Phys. Res., Sect. A **578**, 399 (2007).

[31] Y. Moriwaki, M. Tachikawa, Y. Maeno, and T. Shimizu, Jpn. J. Appl. Phys. **31**, L1640 (1992).

[32] S. Schwarz, Nucl. Instrum. Methods Phys. Res., Sect. A **566**, 233 (2006).

[33] R. G. DeVoe, Phys. Rev. Lett. **102**, 063001 (2009).

[34] L. H. Nguyên, A. Kalev, M. D. Barrett, and B.-G. Englert, Phys. Rev. A **85**, 052718 (2012).

[35] C. Zipkes, L. Ratschbacher, C. Sias, and M. Köhl, New J. Phys. **13**, 053020 (2011).

[36] C. Schneider, M. Enderlein, T. Huber, and T. Schätz, Nat. Photonics **4**, 772 (2010).